MICROBIAL GENOMICS

RESEARCH ARTICLE

Zhang *et al.*, *Microbial Genomics* 2021;7:000549

DOI 10.1099/mgen.0.000549

# Phenotypic and genomic characterization of a *Vibrio parahaemolyticus* strain causing disease in *Penaeus vannamei* provides insights into its niche adaptation and pathogenic mechanism

Xue Zhang[1], Jingfeng Sun[1,*], Feng Chen[1], Hongli Qi[1], Limei Chen[1], Yeong Yik Sung[2], Yadong Huang[3], Aijun Lv[1] and Xiucai Hu[1]

**Abstract**

The virulence of *Vibrio parahaemolyticus* is variable depending on its virulence determinants. A *V. parahaemolyticus* strain, in which the virulence is governed by the *pirA* and *pirB* genes, can cause acute hepatopancreatic necrosis disease (AHPND) in shrimps. Some *V. parahaemolyticus* that are non-AHPND strains also cause shrimp diseases and result in huge economic losses, while their pathogenicity and pathogenesis remain unclear. In this study, a non-AHPND *V. parahaemolyticus*, TJA114, was isolated from diseased *Penaeus vannamei* associated with a high mortality. To understand its virulence and adaptation to the external environment, whole-genome sequencing of this isolate was conducted, and its phenotypic profiles including pathogenicity, growth characteristics and nutritional requirements were investigated. Shrimps following artificial infection with this isolate presented similar clinical symptoms to the naturally diseased ones and generated obvious pathological lesions. The growth characteristics indicated that the isolate TJA114 could grow well under different salinity (10–55 p.p.t.), temperature (23–37 °C) and pH (6–10) conditions. Phenotype MicroArray results showed that this isolate could utilize a variety of carbon sources, amino acids and a range of substrates to help itself adapt to the high hyperosmotic and alkaline environments. Antimicrobial-susceptibility test showed that it was a multidrug-resistant bacterium. The whole-genomic analysis showed that this *V. parahaemolyticus* possessed many important functional genes associated with multidrug resistance, stress response, adhesions, haemolysis, putative secreted proteases, dedicated protein secretion systems and a variety of nutritional metabolic mechanisms. These annotated functional genes were confirmed by the phenotypic profiles. The results in this study indicated that this *V. parahaemolyticus* isolate possesses a high pathogenicity and strong environmental adaptability.

## DATA SUMMARY

Genomic data analysed in this work are available in GenBank and have been described within the article.

## INTRODUCTION

*Penaeus vannamei* is a critical commercial shrimp species cultivated in China and many other countries worldwide [1]. The shrimp farming industry has been deeply affected because of the large scale of mortalities and the lack of effective antibiotics commonly used for shrimp farming [2]. Vibriosis is one of the primary disease problems in cultured shrimp worldwide [3, 4]. *Vibrio* species are part of the natural microflora of wild and cultivated shrimp, and prone to becoming opportunistic pathogens when natural defence mechanisms of the shrimp are suppressed [5].

One of the *Vibrio species*, *Vibrio parahaemolyticus*, is part of the autochthonous microflora in estuarine and coastal marine

Received 26 August 2020; Accepted 25 February 2021; Published 05 May 2021

**Author affiliations:** [1]Tianjin Key Laboratory of Aqua-ecology and Aquaculture, Fisheries College, Tianjin Agricultural University, Tianjin 300384, PR China; [2]Institute of Marine Biotechnology, Universiti Malaysia Terengganu, Kuala Terengganu 21030, Malaysia; [3]Tianjin Hengqian Aquaculture Co. Ltd, Tianjin 300270, PR China.

***Correspondence:** Jingfeng Sun, sun_jf@163.com

**Keywords:** *Penaeus vannamei*; *Vibrio parahaemolyticus*; whole-genome sequencing; niche adaptation; pathogenicity.

**Abbreviations:** AHPND, acute hepatopancreatic necrosis disease; gDNA, genomic DNA; PM, Phenotype MicroArray; TCS, signal transduction system; T2SS, type II secretory system; T3SS, type III secretory system; T4SS, type IV secretory system; T6SS, type VI secretory system.

The GenBank/EMBL/DDBJ accession numbers for the 16S rRNA and gyrase B (*gyrB*) gene sequences are MT799994 and MK560853, respectively. The GenBank/EMBL/DDBJ accession numbers for the sequences of the two chromosomes (chr1 and chr2) and three plasmids (p114-1, p114-2, and p114-3) of *Vibrio parahaemolyticus* TJA114 are CP060087 (chr1), CP060088 (chr2), CP060089 (p114-1), CP060090 (p114-2) and CP060091 (p114-3).

**Data statement:** All supporting data, code and protocols have been provided within the article or through supplementary data files. Eight supplementary tables and two supplementary figures are available with the online version of this article.

environments, and is associated with water, sediment and various aquatic animals ranging from tiny zooplankton to marine mammals [6]. The virulence of *V. parahaemolyticus* is variable depending on the virulence determinants, such as thermostable direct haemolysin (TDH), TDH-related haemolysin (TRH), thermolabile haemolysin (TLH), secretion systems, secretory proteins, prophage, plasmid and other regulatory virulence factors [6, 7]. Recently, *V. parahaemolyticus* has been increasingly reported to cause diseases in *P. vannamei* [8], of which acute hepatopancreatic necrosis disease (AHPND) is the most severe disease currently affecting shrimp aquaculture [9]. Its causative agent is commonly considered as a *V. parahaemolyticus* strain harbouring a 70 kb conjugative plasmid that carries *pirA* and *pirB* genes encoding the binary *Photorhabdus* insect-related toxins A and B (PirAB). Research in AHPND-causing *V. parahaemolyticus*, including pathogenicity, transmission route and genome analysis, has attracted increasing attention from scholars around the world. All AHPND-causing *V. parahaemolyticus* strains so far tested lack some virulence factors such as TDH and TRH [10]. There is an argument that AHPND is not a typical vibriosis infection, but an acute intoxication caused by PirAB toxins delivered directly into the culture water [11]. Phenotypic profiles (morphological, physiological and biochemical characteristics) of different *V. parahaemolyticus* strains are usually similar, while their virulence is variable. The vibriosis of shrimp caused by non-AHPND *V. parahaemolyticus* strains has been occasionally reported in China and other countries [4, 12–14], while the pathogenicity and pathogenesis of the bacteria in the shrimp remain unclear.

In the last decade, whole-genome sequencing has become one of the most promising techniques in clinical microbiology [15]. Following recent improvements in high-throughput sequencing technology, bacterial whole-genome sequencing is now broadly implemented in many areas of research, including detection of virulence genes, prediction of antimicrobial susceptibility, control of infectious diseases and epidemiological investigation [16]. The non-AHPND *V. parahaemolyticus* strains causing shrimp diseases were not completely sequenced, leaving gaps in the understanding of their repertoires.

Recently, diseases with characteristic symptoms of vibriosis in *P. vannamei* occurred in an aquaculture farm in Tianjin, China. The dominant bacterium from the diseased shrimps was identified as a non-AHPND *V. parahaemolyticus* strain. To understand its virulence and adaptation to the external environment, whole-genome sequencing of this *V. parahaemolyticus* strain was conducted, as well as its phenotypic profiles, including pathogenicity, growth characteristics and nutritional requirements, being investigated.

**Impact Statement**

Recently, *Vibrio parahaemolyticus* has been increasingly reported to cause diseases in shrimps. A *V. parahaemolyticus* strain, in which the virulence is governed by the *pirA* and *pirB* genes, can cause acute hepatopancreatic necrosis disease (AHPND) in shrimps. Some *V. parahaemolyticus* that are non-AHPND strains are also important to aquaculture as they can cause shrimp diseases and thus result in huge economic losses, while their pathogenicity and pathogenesis remain unclear. In this study, a non-AHPND *V. parahaemolyticus*, TJA114, was isolated from diseased *Penaeus vannamei* associated with a high mortality. The phenotypic profiles and genomic characteristics of *V. parahaemolyticus* TJA114 revealed that it had a high pathogenicity and strong environmental adaptability. If such pathogens are not taken seriously, they may cause significant economic losses. Our results provide a basis for the deeper understanding of virulence factors and the formulation of better control strategies of *V. parahaemolyticus* infection in shrimps.

## METHODS

### Isolation and identification of the bacteria from diseased shrimps

Diseased and moribund *P. vannamei* (length 9±1 cm) were collected from a shrimp farm in the Jinnan District, Tianjin City, China, where the motility of the cultured shrimp was over 70%. Bacteria were isolated with a sterile loop swabbing over the hepatopancreas of moribund *P. vannamei* and streaked on Luria–Bertani (LB) agar plates. The plates were incubated at 30 °C for 20 h, and dominant uniform bacterial colonies developed. A single dominant bacterial colony was selected and inoculated on the same medium to obtain pure isolate. A pure incubation of an isolate tentatively named TJA114 was stored at −80 °C in LB broth containing sterile glycerol at a final concentration of 15% (v/v).

The bacterial isolate TJA114 was observed under a Leica BMI4000B microscope after Gram staining for morphological study. Physiological and biochemical tests were performed using commercial microtest systems (Binhe Microorganism Reagent, Hangzhou, China) according to the manufacturer's instructions and the indicators under test are shown in Table 1.

The 16S rRNA and gyrase B (*gyrB*) genes were used for the molecular identification of the isolate TJA114. Total genomic DNA (gDNA) was extracted from isolate TJA114 using a bacterial genomic DNA extraction kit (TaKaRa, Tokyo, Japan). The 16S rRNA and *gyrB* genes were amplified by PCR with the primers shown in Table S1 (available in the online version of this article) [17, 18]. Amplification conditions were set up according to a previous report by Han *et al.* [19]. Then, the PCR amplification products were electrophoresed in 1% agarose gels. A BLAST search for 16S rRNA and *gyrB* gene sequences was carried out with the National Center for Biotechnology Information website. The alignment was performed using CLUSTAL W and phylogenetic trees were reconstructed using the neighbour-joining algorithm with 1000 bootstrap replicates in the software MEGA 6.0. This isolate was also subjected to the detection of some virulence factor genes, including *tdh*, *trh*, *tlh*, *pir* and cholera toxin

**Table 1.** Physiological and biochemical characteristics of the isolate TJA114

| Characteristic | Reaction | Characteristic | Reaction |
|---|---|---|---|
| Gelatin liquefaction | – | Sorbitol | – |
| Methyl red test | + | Utilization of: | |
| Motility | + | Malonate | – |
| Nitrate reduction | + | Starch | + |
| Oxidative/ fermentative | F | Hydrolysis of: | |
| Voges–Proskauer test | + | Urea | + |
| Acid formation from: | | Growth in: | |
| Adonitol | – | 0% NaCl peptone water | – |
| Arabinose | + | 7% NaCl peptone water | + |
| Glucose | + | 10% NaCl peptone water | – |
| Inositol | – | 37°C | + |
| Lactose | + | Production of: | |
| L-Rhamnose | – | Arginine dihydrolase | – |
| Maltose | + | $H_2S$ | – |
| Mannitol | + | Lysine decarboxylase | + |
| Raffinose | – | Ornithine decarboxylase | + |
| Sucrose | – | Oxidase | + |

transcriptional activator (*toxR*), by using PCR with their respective specific primers listed in Table S1 [20–22].

## Recursive infection experiment

Healthy *P. vannamei* (length 7±1 cm) were provided from Tianjin Hengqian Aquaculture Co. Ltd. and acclimatized in the laboratory in three glass aquariums (20 shrimps per tank) filled with 200 l filtered tap water with a salinity of 3 p.p.t. at 26±0.5 °C for 2 weeks. Dissolved oxygen was maintained at about 8 mg $l^{-1}$ and nitrite concentration was kept below 0.05 mg $l^{-1}$ by using air stones and replacing one-third of the water in every aquarium every day. Shrimps were fed with commercial compound feed (Sanfapulin Feed, Tangshan, China) at 8.00 am and 5.00 pm every day.

After acclimatization for 2 weeks, ten shrimps were randomly selected from each aquarium and moved into three polyethylene boxes containing 4 l saltwater taken from the previously used aquarium, which represented three separate groups (group 1, 2 and 3). Shrimps in group 1 were infected by immersion with the TJA114 isolate at a final concentration of $1\times10^8$ c.f.u. $ml^{-1}$, those in group 2 at $1\times10^7$ c.f.u. $ml^{-1}$. Group 3 was used as an uninfected control. Two hours later, all shrimps in the three groups were transferred back to the original three aquariums, and the health conditions and clinical signs of the infected shrimps were observed. The first five moribund shrimps from the two infected groups and five shrimps from the control group were subjected to bacterial isolation from the hepatopancreas on LB agar plates. After that, these plates were incubated at 30 °C for 20 h. Single colonies from the plates were randomly selected and subjected to detection of *V. parahaemolyticus* targeting the *toxR* gene by using PCR with a pair of specific primers (Table S1).

## Histological examination

The histological examination of the hepatopancreas, intestines and gills from the diseased shrimps artificially infected with the isolate TJA114 was performed as previously described [19]. Formalin-fixed tissues were dehydrated in graded alcohols, and embedded in paraffin wax. Samples were sectioned with a Thermo Microm HM 355S microtome (Thermo Fisher Scientific, Waltham, MA, USA) into 5 µm thick slices. The sections were stained with haematoxylin and eosin, and then observed under a light microscope (Leica, Berlin, Germany).

## Genome sequencing and annotation

The TJA114 isolate was cultured and harvested at the late-exponential growth phase. Its gDNA was extracted with the SDS method and purified with a genomic DNA preparation kit (Thermo Fisher Scientific, Waltham, MA, USA). The DNA obtained was detected by the agarose gel electrophoresis and quantified by a Qubit 2.0 fluorometer (Invitrogen, Carlsbad, CA, USA). Fragmented gDNA was used for library construction with a 10 kb PacBio SMRT bell library preparation kit (Pacific Biosciences, Menlo Park, CA, USA) and sequenced by the single-molecule real-time (SMRT) technology on the PacBio RSII sequencing platform (Pacific Biosciences, Menlo Park, CA, USA) with 100× coverage. At the end, low-quality reads were filtered out with SMRT Link version 5.0.1 (Pacific Biosciences, Menlo Park, CA, USA) and the filtered reads were *de novo* assembled [23]. phiSpy version 2.3 was used for the prophage prediction [24].

## Gene function analysis and identification of virulence genes

A whole-genome BLAST search (*E* value $<1\times10^{-5}$, minimal alignment length percentage larger than 40%) was performed against the Kyoto Encyclopedia of Genes and Genomes (KEGG) [25], Clusters of Orthologous Groups of proteins (COG) and Non-Redundant protein (NR) databases [26] to predict gene functions. EffectiveT3 version 1.0.1 [27] was used to analyse type I–VII secretion systems. The Virulence Factor Database (VFDB) and Comprehensive Antibiotic Research Database (CARD) were applied for identification of the virulence and resistance factors, respectively [28, 29].

### Antimicrobial-susceptibility test

Susceptibility of the isolate TJA114 to antibiotics was determined on LB agar plates using the Kirby–Bauer disc diffusion method [19]. The antimicrobial agents (Hangzhou Microbial Reagent, Hangzhou, China) tested are shown in Table 2. The zones of inhibition were measured after 16–18 h incubation at 30 °C and the sensitivity was determined according to the manufacturer's instructions (Hangzhou Microbial Reagent, Hangzhou, China).

### Growth characteristics

The effect of pH on the growth of the isolate TJA114 was studied at pH values 6, 7, 8, 9 and 10 in a modified basic medium (MBM; 10 g tryptone $l^{-1}$, 5 g yeast extract powder $l^{-1}$) under 30 p.p.t. salinity at 30 °C; the effect of salinity at 10, 25, 30, 40 and 55 p.p.t. was studied in MBM with a pH value of 7 at 30 °C; the effect of temperature was studied at 23, 26, 30 and 37 °C in MBM with a pH value of 7 and salinity of 30 p.p.t. The pH was adjusted to the desired values with NaOH (1 mol $l^{-1}$) or HCl (1 mol $l^{-1}$) before the medium was sterilized by autoclaving. All flasks containing 200 ml prepared broth medium were inoculated with 0.2 ml bacterial suspension ($OD_{600}$ 2) [30] and cultured at 150 r.p.m. Then, growth was monitored for 200 h by measuring the optical density at 600 nm every 2 h with an ultraviolet spectrophotometer UV-5800 (Metash Instruments, Shanghai, China). The artificial growth curves were drawn according to a report by Han *et al.* [19].

### Phenotype MicroArray (PM) assays

PMs (Biolog, San Francisco, CA, USA) are a high-throughput technology for simultaneous testing of a large number of cellular phenotypes. The tests were conducted in accordance with standard protocols recommended by Biolog for *Escherichia coli* and other Gram-negative bacteria [31]. The test components of PM 01, PM 02, PM 09 and PM 10 are shown in Table S2. All the substrates tested were pre-dispensed and dried in 96-well plates, requiring only inoculation with bacteria suspended in a buffer containing a Dye Mix D (Biolog, San Francisco, CA, USA).

For preparation of the PM inoculating fluid of IF-0+dye, 0.36 ml Dye Mix D and 4.64 ml sterile water was added to 25 ml IF-0 GN/GP Base inoculating fluid (1.2×) (Biolog, San Francisco, CA, USA). For preparation of the PM inoculating fluid of IF-10+dye, 0.3 ml Dye Mix D and 4.7 ml sterile water was added to 25 ml IF-10 GN Base inoculating fluid (1.2×) (Biolog, San Francisco, CA, USA). The bacteria cultured overnight on LB agar plates at 30 °C were suspended in 30 ml IF-0+dye PM inoculating fluid and the cell density was adjusted on a Biolog turbidimeter to obtain an 85% transmittance (T) bacterial suspension. Each well of the PM 01 and PM 02 plates was inoculated with 100 µl of this bacterial cell suspension. For PM 09 and PM 10 plates, 0.15 ml of this 85% T bacterial suspension was transferred into the prepared 30 ml IF-10+dye PM inoculating fluid and mixed completely to make a 200-fold-diluted 85% T bacterial suspension. Then, 100 µl of this bacterial suspension was inoculated into each well of the PM 09 and PM 10 plates. All the plates were incubated in an OmniLog (Biolog, San Francisco, CA, USA) for 48 h, with readings taken every 1 h. Data analysis was performed using Kinetic and Parametric software (Biolog, San Francisco, CA, USA). Phenotypes were determined based on the kinetic curve of dye formation.

## RESULTS

### Isolate TJA114 is a non-AHPND *V. parahaemolyticus*

A dominant bacterium was isolated from the hepatopancreas of moribund *P. vannamei* and named as TJA114. This bacterial isolate was a Gram-negative short rod-shaped bacterium. Its colonies appeared circular, convex, glossy and opaque on LB agar after 20 h incubation, and its physiological and biochemical characteristics are summarized in Table 1. The isolate TJA114 did not grow in salt-free pancreatic peptone water. It was motile and fermented, able to hydrolyse starch and reduce nitrate. Moreover, it was positive for production of oxidase, lysine decarboxylase and ornithine decarboxylase, but negative for production of $H_2S$ and arginine dihydrolase. These characteristics were in accordance with those of a previously reported *V. parahaemolyticus* [32]. The sequences of the 16S rRNA and *gyrB* genes were, respectively, 1443 and 1149 bp in length, and showed the highest identity of 99.79% with *V. parahaemolyticus* JQ9047331.1 and 99.60% with *V. parahaemolyticus* JF907570.1, respectively. Neighbour-joining phylogenetic trees based on these two sequences showed that the TJA114 isolate was clustered in the *V. parahaemolyticus* group (Fig. 1a, b). This isolate was subjected to the detection of five virulence genes, and found to be negative for *pir*, *tdh* and *trh* genes but positive for *tlh* and *toxR* genes (Fig. 1c). Taking these results together, the TJA114 isolate is a non-AHPND *V. parahaemolyticus* [33].

### Plasmid features of the TJA114 isolate reveal a strong adaptability to environment

The filtered reads of TJA114 isolate were *de novo* assembled into a genome sequence. The genome sequence included two circular chromosomes (chr1 1810082 bp, G+C content=45.45 mol%, VP_GM000001-1668; chr2 3522430 bp, G+C content=45.05 mol%, VP_GM001864-5095), and three plasmids named p114-1 (120965 bp, G+C content=46.03 mol%, VP_GM001669-1808), p114-2 (36923 bp, G+C content=51.62 mol%, VP_GM001809-63) and p114-3 (78477 bp, G+C content=45.35 mol%, VP_GM005096-5185). The N50 read length and genome size of *V. parahaemolyticus* TJA114 were 3531973 and 5568877 bp (5185 genes, G+C content=46.10 mol%), respectively.

The comparative sequence analysis between the isolate TJA114 and the *V. parahaemolyticus* PB1937, which was the only completely sequenced isolate among the AHPND-causing *V. parahaemolyticus* strains, showed that their chromosomes had good collinearity overall, and their differences were mainly reflected in the plasmids (Fig. 2a). The sequence of the plasmid p114-1 was not annotated in *V. parahaemolyticus* PB1937. This plasmid harbouring four conjugative

**Table 2.** Drug sensitivity of the isolated strain TJA114

| Group | Name | Drug content (μg per disc) | Bacteriostatic ring (mm)* | Sensitivity† |
|---|---|---|---|---|
| *β*-Lactams | Amoxicillin/clavulanic acid | 10 | 8 | R |
| | Ampicillin | 10 | 7 | R |
| | Ampicillin/sulbactam | 10 | 20 | S |
| | Cefotaxime | 30 | 30 | S |
| | Cefradine | 30 | 16 | I |
| | Ceftazidime | 30 | 30 | S |
| | Ceftriaxone | 30 | 27 | S |
| | Cephalexin | 30 | 14 | R |
| | Imipenem | 10 | 32 | S |
| | Meropenem | 10 | 34 | S |
| | Oxacillin | 1 | 7 | R |
| | Penicillin G | 10 | 7 | R |
| Aminoglycosides | Amikacin | 30 | 14 | R |
| | Gentamicin | 10 | 15 | S |
| | Kanamycin | 30 | 16 | R |
| | Neomycin | 30 | 20 | I |
| | Streptomycin | 10 | 17 | S |
| Chloramphenicols | Chloramphenicol | 30 | 24 | S |
| Macrolides | Azithromycin | 15 | 26 | S |
| | Erythromycin | 15 | 28 | S |
| Nitrofurans | Furazolidone | 300 | 14 | R |
| | Nitrofurantoin | 300 | 15 | I |
| Quinolones | Ciprofloxacin | 5 | 22 | S |
| | Enoxacin | 10 | 24 | S |
| | Levofloxacin | 5 | 28 | S |
| | Nalidixic acid | 30 | 22 | S |
| | Norfloxacin | 10 | 19 | S |
| | Ofloxacin | 10 | 24 | I |
| Sulfonamides | Trimethoprim/sulfamethoxazole | 24 | 20 | S |
| Tetracyclines | Doxymycin | 30 | 10 | R |
| | Minocycline | 30 | 14 | R |
| | Tetracycline | 30 | 8 | R |
| Others | Clindamycin | 2 | 8 | R |
| | O/129 | 150 | 25 | S |
| | Polymyxin B | 300 | 10 | I |
| | Rifampicin | 5 | 19 | I |
| | Vancomycin | 30 | 7 | R |

*The diameter of the inhibition zone includes the 7 mm drug disc.
†S, Susceptible; I, moderately susceptible; R, resistant.

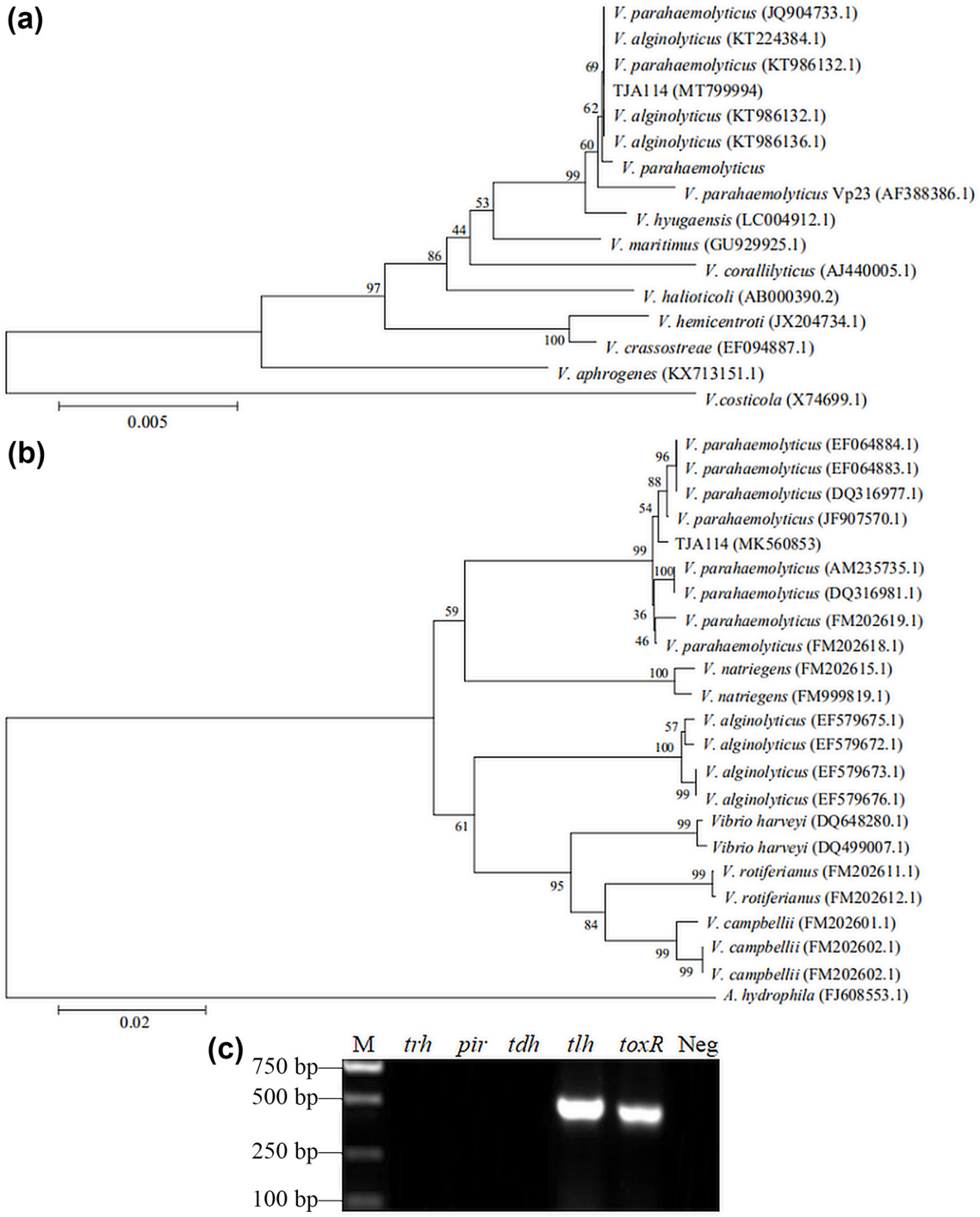


**Fig. 1.** Molecular identification and virulence gene detection of the isolate TJA114. (a) Neighbour-joining phylogenetic tree based on the 16S rRNA gene sequence. The 16S rRNA gene of *Salinivibrio costicola* (X74699.1) was used as the outgroup. (b) Neighbour-joining phylogenetic tree based on the *gyrB* gene sequence. The *gyrB* gene of *Aeromonas hydrophila* (FJ608553.1) was used as the outgroup. The numbers next to the branches indicate percentage values for 1000 bootstrap replicates. The scale bar represents the number of substitutions per site. (c) The agarose gel electrophoresis did not show the *trh*, *tdh* and *pir* genes, but did show *tlh* and *toxR* genes from PCR products. M, Marker; Neg, negative control.

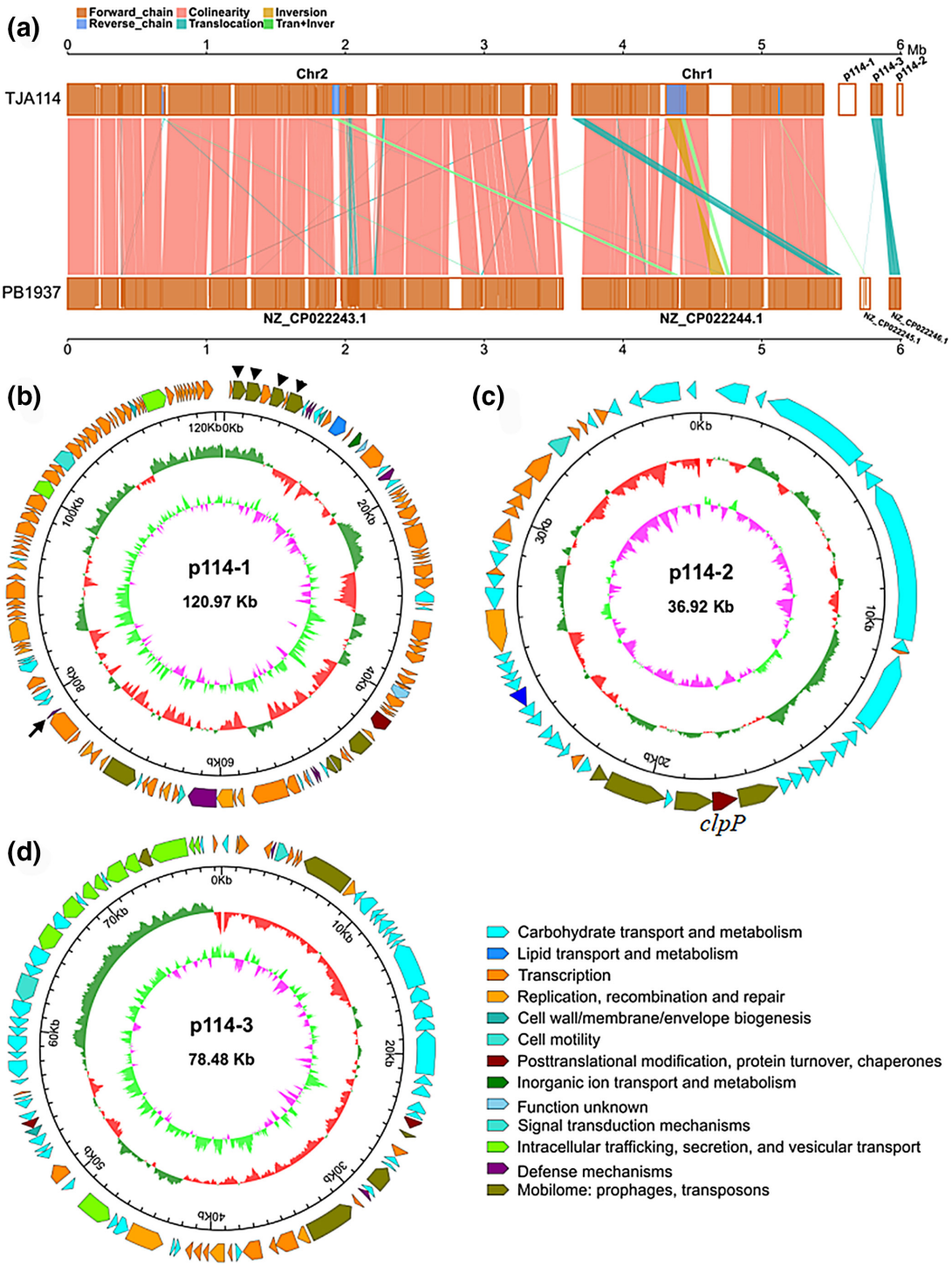


**Fig. 2.** The genomic analysis and plasmid circular atlases of the isolate TJA114. (a) Synteny blocks of the genomes between the isolate TJA114 and *V. parahaemolyticus* PB1937. The box at the top represents the genome of the isolate TJA114, and the box at the bottom represents the strain *V. parahaemolyticus* PB1937. In this, orange represents the forward strand of the genome, and blue represents the reverse strand of the genome. The height of the filled colour in the box indicates the similarity of the match, and full fill indicates a similarity of 100%. (b) Circular atlas of plasmid p114-1 (arrow, bacteriocin immunity protein; arrowheads, conjugative proteins). (c) Circular atlas of plasmid p114-2. (d) Circular atlas of plasmid p114-3. (b–d) Circle 1 (from outside to inside), coding genes of COG functional annotation (clockwise arrows, predicted coding sequences on the positive strand; anticlockwise arrows, predicted coding sequences on the negative strand); circle 2, coordinates of genome sequence positions; circle 3, G+C percentage content (green, above average G+C content; red, less than or equal to the average); circle 4, GC skew (light green, (G–C)/(G+C) >0; purple (G–C)/(G+C) <0).

**Table 3.** Top five plasmids with the highest identity with the plasmid p114-2 (36924 bp) from the isolate TJA114

| Subject ID | Subject length (bp) | Query cover (%) | *E* value | Identity (%) | Description |
|---|---|---|---|---|---|
| NC_010529.1 | 557200 | 0.07 | 0.59 | 96.3 | *Cupriavidus taiwanensis* str. LMG19424 plasmid pRALTA |
| NC_005871.1 | 80033 | 0.13 | 2.30 | 100 | *Photobacterium profundum* SS9 plasmid 1 |
| NC_006258.1 | 5987 | 0.11 | $3.00\times10^{-6}$ | 95 | *Rhodococcus erythropolis* plasmid pRE8424 |
| NZ_CP017585.1 | 25681 | 0.11 | 0.01 | 90.48 | *Pantoea stewartii* subsp. *stewartii* DC283 plasmid pDSJ04 |
| NZ_CP007239.1 | 1614950 | 0.06 | 0.15 | 100 | *Ensifer adhaerens* OV14 plasmid pOV14b |

protein genes (Fig. 2b, arrowheads) indicated that p114-1 was probably obtained by conjugation. A bacteriocin immunity protein gene, previously reported in *Streptococcus mutans*, can help bacteria resist the effects of antimicrobial agents [34]. This gene was also identified in the plasmid p114-1 (Fig. 2b, arrow) and is probably beneficial for *V. parahaemolyticus* TJA114 resistance to antimicrobial substances. The plasmid p114-2 in the isolate TJA114 has never been reported in *Vibrio* (Table 3). It had an obviously different G+C content (51.62mol%), compared with that of the genome (46.10mol%), and harboured a *clpP* gene (VP_GM001827) located on a prophage (Fig. 2c, dark green). These features indicated it was probably a newly obtained plasmid. The existence of *clpP* gene in this plasmid was expected to contribute greatly to the regulation of environmental adaptation and cell division, according to the previous studies on ClpP function in *Bacillus subtilis* [35] and *Legionella pneumophila* [36]. The plasmid p114-3 had the highest identity with a plasmid p1987-2 (NZ_CP022246.1) existing in *V. parahaemolyticus* PB1937 (100% query cover, *E* value=0) (Fig. 2a). It contained genes related to the type IV secretory system (T4SS; Fig. 2d, light green) that is mainly responsible for horizontal gene transfer. Specifically, TJA114 was not aligned to the virulence plasmid p1937-1 (NZ_CP022245.1), which harboured *pirAB* genes and was found in *V. parahaemolyticus* PB1937 [37] (Fig. 2a). This indicated the non-AHPND TJA114 strain might have different pathogenicity, compared with the AHPND-causing *V. parahaemolyticus*. The two plasmids p114-1 and p114-2 existing in the isolate TJA114 but not the *V. parahaemolyticus* PB1937 strain indicated the former probably had stronger adaptability to environment than the latter.

## Genomic evidence corresponds to a strong aggressiveness

Invasion is a prerequisite for a pathogenic bacterium to cause infection, and is governed by the abilities of motility, adhesion and biofilm formation and the functions of extracellular proteases and haemolysin [6]. Complete flagella and lateral flagella systems were identified in the TJA114 isolate (Table S3). This indicated that TJA114 might possess dual flagellar systems to adapt for movement under different circumstances; thus, facilitating the initial steps of bacterial invasion into the host cell [38]. We identified some genes encoding type IV pilus biogenesis proteins PilABCD, twitching motility protein PilT and mannose-sensitive haemagglutinin (MSHA type IV pilus) synthesis proteins MshACDEFGHIJKLMNOPQ (Table S3), which are the main factors related to the adhesion of *V. parahaemolyticus* [39]. In addition, we identified the genes of the immunogenic lipoprotein A (IlpA) and multivalent adhesion molecule MAM7 (Table S3), which benefit high-affinity binding to host cells during the early stages of infection [40, 41].

The TJA114 genome contained the genes of outer-membrane protein U (*ompU*), *toxR* and determinants *cpsABCDEFGHIJ* (Table S3). Their coding products may contribute to biofilm formation of the *V. parahaemolyticus*, and confer a selective advantage by increasing the ability of the bacterium to protect itself from host immunity and antimicrobial attack [42]. The genome encoded 17 putative secreted proteases, such as serine protease, collagenase, chitinase, lipase and peptidase, probably involved in destruction of the host barrier (Table S4). These putative secreted proteases likely function in the destruction of the structure of collagen, chitin, lipid and protein; thus, interfering in the metabolism of these substances in organs such as the hepatopancreas, gastrointestinal tract and gills, which are mainly the target organs attacked by *V. parahaemolyticus* [43].

The *tlh* gene but not the *tdh* and *trh* genes was found in the TJA114 genome (Table S4). Three kinds of haemolysin TDH, TRH and TLH, encoded by *tdh*, *trh* and *tlh* genes, responsible for the haemolytic activity are usually present in clinical *V. parahaemolyticus* strains causing human diseases [6]. The absence of *tdh* and *trh* genes in the isolate TJA114 could not exclude the probability of haemolysis when invading hosts since haemolysin TLH might confer the haemolytic activity in the presence of lecithin, which is present in most living organisms [44]. The genes VP_GM002728–VP_GM002730 were annotated as three ferrous iron transport proteins, FeoA, FeoB and FeoC. These three proteins constituted a $Fe^{2+}$ uptake system (Fig. 3), which was reported to be related to the pathogenicity of *Vibrio* [45]. Moreover, the genes of six TonB-dependent outer-membrane iron receptors and a siderophore-mediated iron uptake system (Fig. 3) were speculated to participate in the process of obtaining the necessary iron in the isolate TJA114. Furthermore, the annotated haem transport system encoded by VP_GM004180-83 (Fig. 3) may transport extracellular haem to the cytoplasm. Additionally, two haem oxygenase genes (VP_GM000691, VP_GM000782) were identified, indicating that haem may be oxidized to biliverdin, carbon monoxide (CO) and ferrous ions [46].

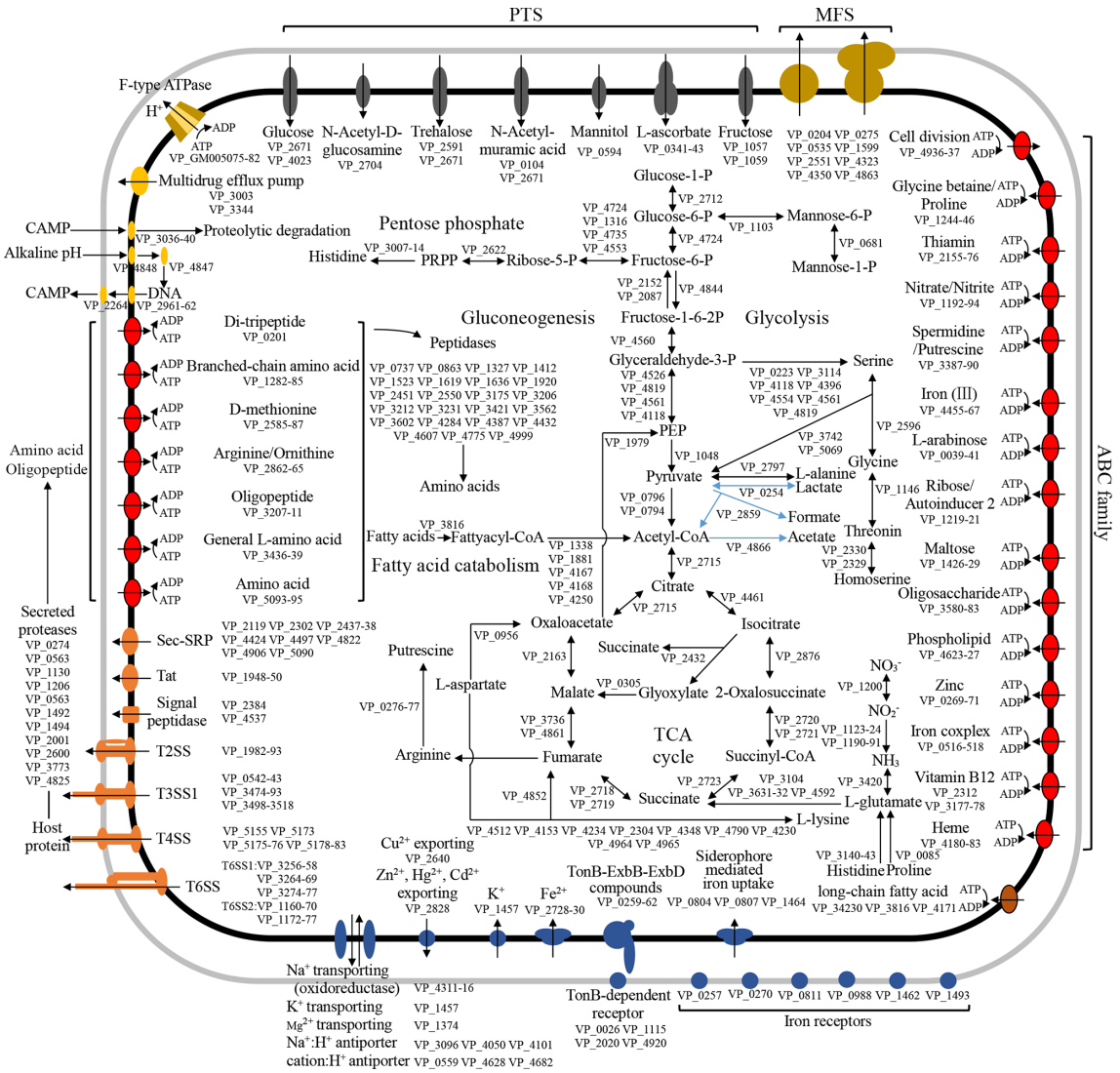


**Fig. 3.** Overview of metabolism and transport in *V. parahaemolyticus* TJA114. Different colours and shapes distinguish different transport families: phosphotransferase system (PTS), grey; the major facilitator superfamily (MFS), orange/brown; ABC family, red; long chain fatty acid transport, red/brown; ion transport, blue; secretion systems, orange; drug efflux, golden yellow; F-type ATPase, orange/brown and golden yellow. Arrows indicate the direction of transport.

## Secretory systems of the isolate TJA114 play an important role in cytotoxicity and horizontal gene transfer

Secretion systems are of great significance for virulence by directing toxins to the bacterial surface or host cells. Among these systems, the sec-dependent (Sec) transport system, twin-arginine transport (Tat) system, type II secretory system (T2SS), type III secretory system 1 (T3SS1), T4SS and type VI secretory system (T6SS) were identified in the genome of TJA114 isolate (Fig. 3).

The integrated Sec, Tat transport system and T2SS were identified (Fig. 3), implying that TLH and other extracellular protein toxicity factors may be released through T2SS and act on hosts, leading to cell damage and disease [47, 48]. T3SS1, a T3SS located in the chr1 of the *V. parahaemolyticus*, possesses several effectors such as VPA0450 (VP_GM000542), VopQ (VP_GM003498), VopR (VP_GM003500) and VopS (VP_GM003502), and specific chaperone proteins VecA (VP_GM003499) and VPA0451 (VP_GM000543), indicating that TJA114 may have the ability to induce autophagy of host cells and macrophage death [49–52]. The T3SS2 usually encoding the *trh* and/or *tdh* genes was not annotated in the genome of TJA114, indicating that this strain may not secrete enterotoxin [53, 54]. This secretory system is usually present in most clinical *V. parahaemolyticus* causing human diseases, while absent in most environmental *V. parahaemolyticus* [6]. TJA114 harbours a complete set of components of T4SS such as *trbBCDEFGHIJLN* and *traD* (VP_GM005179,

VP_GM005183–81, VP_GM005176–73, VP_GM005180, VP_GM005178, VP_GM005155 and VP_GM001799). The secretory system T4SS was reported to function in mediating the horizontal transfer of resistance genes or virulence genes [55]. Since T6SS1 can provide a competitive advantage to *V. parahaemolyticus* when encountering the commensal flora of the host [37, 56], the presence of T6SS1 in the isolate TJA114 may contribute to its niche competitiveness. T6SS2, which could be involved in the autophagic response in host cells in a previously reported *V. parahaemolyticus* [57], was also found in the isolate TJA114.

## Metabolism diversity in the isolate TJA114 reflects the extensive available nutrients

To understand the metabolic characteristics of TJA114, we present a genome-scale metabolic model of the isolate (Fig. 3). Phosphotransferase systems for transport and metabolism of specific carbohydrate such as glucose, *N*-acetyl-D-glucosamine, trehalose, *N*-acetyl-muramic acid, mannitol, L-ascorbate and fructose were found in the TJA114 genome (Fig. 3), which were expected to play a major role in transport and metabolism of energy [58]. The important metabolic pathways for the energy supply of the organism including complete gluconeogenesis, glycolysis, pentose phosphate and tricarboxylic acid (TCA) cycle (Fig. 3) were probably beneficial for the TJA114 to perform catabolism in the case of normal or carbon source constraints. The pathways of pyruvate conversion to lactate, formate and acetate (Fig. 3, blue arrows) might indicate the adaptation of this *V. parahaemolyticus* isolate to the specific living environments of organic infection. This adaptation is in accordance with the facultative anaerobic lifestyle of *V. parahaemolyticus* in intracellular niches [59].

The TJA114 genome possessed catabolic pathways of extensive amino acids, such as histidine, arginine, alanine, aspartate, glycine, serine and threonine, oligopeptides, oligosaccharides, and fatty acids (Fig. 3), which could be from the host protein degraded by a variety of peptidases of this bacterial strain, benefitting provision of sources of carbon, nitrogen and energy for growth. Moreover, integrated transport and metabolism pathways of nitrate/nitrite suggested the ability of this bacterial isolate to utilize an inorganic nitrogen source.

A complete respiratory chain and an ATP synthetase complex (VP_GM005075-82) were found in the genome-scale metabolic model. The genome encoded a variety of dehydrogenases ($n$=83, Table S5) and many reductases ($n$=67, Table S5). The dehydrogenases might enable the isolate to use a variety of electron donors, such as NADH, malate, lactate, formate, proline, isocitrate, succinate and acyl-CoA; while the reductases might enable it to use alternative electron acceptors, such as fumarate, nitrate, nitrite, dimethyl sulfoxide, arsenate, tetrathionate and trimethylamine-*N*-oxide. The utilization of these electron donors and acceptors probably contributes to respiration for supporting the bacterium's facultative anaerobic lifestyle in host niches.

## Genomic evidence suggests that the isolate TJA114 can cope with a variety of environmental stresses

In the isolate TJA114, an array of sigma factors and anti-sigma factors were identified (Table S6), including four *rpoE* genes, two *flgM* genes, a *fliA* gene, a *rpoS* gene, three sigma-E factor negative regulatory protein genes *rseABC* and many sigma-54 transcriptional regulator genes. The sigma and anti-sigma factors are responsible for modulating various virulence traits [60], heat-shock response [61], flagellar biosynthesis [62], the stress resistance of acid, oxidation, hyperosmolarity and temperature [63]; thus, probably laying the foundation for this strain to respond to various environmental or host stimuli and drive the expression of related functional genes for cellular fitness [59].

Chaperone genes including five cold-shock protein genes, eight heat-shock protein genes, two *dnaJ* genes and a *dnaK* gene were identified in the strain TJA114 (Table S7). The existence of these chaperone genes indicates that the strain might have strong resistance to various environmental stresses such as low or high temperature, high salt and a heavy metal environment [64]. In addition, this isolate also possessed a phage shock protein (Psp) system, PspABCEF, which could help it to respond to phage induction and various membrane stimuli (Table S7). The genes responsible for the synthesis and uptake of several compatible solutes (osmolytes) such as ectoine, lysine, betaine and proline were identified, including *ectABC*, *cadABC*, *bcT*, *betABI* and *proVWX* (Table S7). These osmolytes were reported to benefit bacterial resistance to the high salinity, heat, acid, freezing and drying [65–67].

Genes encoding antioxidants for dealing with oxidative stress [68] were identified, including superoxide dismutase genes *sod1* and *sod2*, catalase gene *cat*, bifunctional catalase-peroxidase gene *katG*, peroxiredoxin gene *ahpC*, glutathione peroxidase gene *gpx*, alkyl hydroperoxide reductase gene *ahpF*, coproporphyrinogen III oxidase gene *hemF* and hydrogen peroxide-inducible genes activator gene *oxyR* (Table S7).

The isolate TJA114 encoded a cationic antimicrobial peptides (CAMP) resistance pathway (Fig. 3, golden yellow) that may degrade or/and pump out CAMP produced by the host to resist pathogenic micro-organisms. Besides, many specific drug- and multidrug-resistant genes, such as tetracycline-resistant efflux pump gene *tet35* (VP_GM003003), multidrug-resistant efflux pump gene *norM* (VP_GM003344), multidrug-resistant protein genes *emrB* (VP_GM000204), *emrD* (VP_GM000275) and *mdtL* (VP_GM000535, VP_GM001599), nitroreductase gene *nfnB* (VP_GM001616), and metallo-$\beta$-lactamase family protein K07576 gene (VP_GM002081), were also present in the genome.

In the genome of the isolate TJA114, several two-component signal transduction systems (TCSs; phosphoglycerate and trimethylamine-*N*-oxide) were identified, containing 19 sensor histidine kinases (HK) genes and 21 response regulator (RR) genes (Table S8). The phosphoglycerate TCS was encoded by *pgtA* and *pgtB* genes, and the trimethylamine *N*-oxide TCS was encoded by *torR* and *torS* genes (Table S8). These two TCSs

probably contribute to the development of an intracellular niche, since phosphoglycerate and trimethylamine-*N*-oxide are extensively present in the host cells. The two TCSs, ArcB–ArcA (encoded by *arcB* and *arcA* genes) and CitA–CitB (encoded by *citA* and *citB* genes), have been reported to be associated with the switch from aerobic to anaerobic growth in *E. coli* [64]. These two TCSs were also identified in the isolate TJA114 (Table S8), indicating that this isolate could maintain both aerobic and anaerobic lifestyles.

Taken together, the presence of these genes encoding various stress adaptation factors probably helps the isolate TJA114 to overcome temperature fluctuation, pH changes, osmolarity variation, oxidative stress and antibacterial agents, as well as the responsive reactions of hosts, in the process of survival, invasion and causing diseases.

## Antimicrobial-susceptibility test confirms the isolate TJA114 as a multidrug-resistant bacterium

The antimicrobial-susceptibility results showed that the isolate TJA114 was sensitive to chloramphenicols such as chloramphenicol, macrolides such as azithromycin and erythromycin, and quinolones such as ciprofloxacin, enoxacin, levofloxacin, nalidixic acid, norfloxacin and ofloxacin (Table 2). Nevertheless, it showed varying degrees of resistance to different kinds of antibiotics, distributing in *β*-lactams (amoxicillin/clavulanic acid, ampicillin, cefradine, cephalexin, oxacillin and penicillin G), aminoglycosides (amikacin, kanamycin and neomycin), nitrofurans (furazolidone and nitrofurantoin) and tetracyclines (doxymycin, minocycline and tetracycline) (Table 2). These results showed that this isolate was a multidrug-resistant *V. parahaemolyticus* and confirmed the multidrug-resistant genes identified in its genome.

## Isolate TJA114 is the aetiological agent

In order to determine whether the *V. parahaemolyticus* TJA114 was the aetiological agent, we carried out a recursive infection in *P. vannamei*. The bacterial colonies from the hepatopancreas of artificially infected shrimps showed the same characteristics with the TJA114 isolate, while no colonies were observed from the uninfected shrimps. The results of detection for the *toxR* gene of *V. parahaemolyticus* from the selected ten colonies that were isolated from the hepatopancreas of artificially infected shrimps by using PCR with specific primers (Table S1) were positive (Fig. 4a). The pathological lesions in the hepatopancreas, intestines and gills from the artificially infected shrimps were consistent with the natural diseased case. In the hepatopancreas, haemocyte infiltration (Fig. 4b), enlarged intertubular spaces (Fig. 4c), hypervacuolization (Fig. 4d), karyopyknosis (Fig. 4e) and sloughing of hepatopancreas cells from the basement membrane (Fig. 4f) were observed. In the intestine, the epithelium collapsed and fell off into the intestinal lumen, and proliferating cells were found on the intestinal basement membrane (Fig. 4g). In the gills, swelled filaments and separated epithelial cells from gill membranes were observed (Fig. 4h). The control shrimps presented no obvious pathological lesions.

Taken together, these results for re-isolation of the *V. parahaemolyticus* isolate, PCR detection of the *toxR* gene and pathological lesions were in accordance with Koch's postulate; thus, confirming the isolate TJA114 as the aetiological agent for the disease in *P. vannamei*.

## Artificial growth curves reveal the adaptation of the isolate TJA114 to different environmental conditions

The cultured *V. parahaemolyticus* TJA114 could grow and exhibited a similar growth rate in the different respective conditions of salinity of 10–55 p.p.t., temperature of 23–37 °C and pH of 6–10 (Fig. 5a–c). And there was a long plateau phase and considerable final concentrations at the various tested salinity, pH and temperature conditions (Fig. 5a–c). Of note, a secondary growth at 80–100 h (Fig. 5a–c) and a short latent phase (Fig. S1) were observed on its growth curves.

## Isolate TJA114 can utilize a variety of carbohydrates, amino acids and a range of substrates

To verify the substrate utilization, compatible osmolytes, and the adaptation to acid and base environments of the isolate TJA114, we conducted Biolog PM assays with the plates PM 01, PM 02, PM 09 and PM 10 for the phenotypic characterization. The isolate TJA114 utilized the majority of the carbon sources (Fig. S2a–b, Table S2). In addition, it could grow under the NaCl concentration of 1–7% (Fig. S2c, Table S2), which is similar to the results of the artificial growth curve at different salinity levels (Fig. 5a). When the 6% NaCl combined with some substrates, including betaine, *N-N* dimethyl glycine, sarcosine, dimethyl sulphonyl propionate, MOPS, ectoine, choline, phosphorylcholine, creatine, L-carnitine, KCl, L-proline, *N*-acetyl-L-glutamine, *β*-glutamic acid, γ-amino-*N*-butyric acid, glutathione, glycerol, trehalose, trimethylamine-*N*-oxide, trimethylamine, octopine or trigonelline, a higher final concentration of the isolate TJA114 (Fig. S2c, Table S2) was observed than that without these substrates (control well, 6% NaCl) (Fig. S2c, A07; Table S2), indicating that these substrates could relieve the osmotic pressure for its growth. Many of the transport systems of these substrates were identified in the KEGG metabolic pathway (Fig. 3).

The isolate TJA114 grew at pH 5–10 and grew well at pH 5.5–10 (Fig. S2d, Table S2), this was consistent with its artificial growth curves at different pH values (Fig. 5c). At pH 4.5, the presence of 5-hydroxy-tryptophan induced the growth reversed, compared to the negative control (control well, pH 4.5) (Fig. S2d, A03; Table S2), indicating this substrate could help the isolate resist the acid stress. At pH 9, the presence of some substrates including L-alanine, L-arginine, L-asparagine, L-aspartic acid, L-glutamic acid, L-glutamine, glycine, L-lysine, L-methionine, L-proline, L-serine, L-threonine, L-valine, hydroxy-L-proline, L-ornithine, anthranilic acid or L-norvaline resulted in a faster approach to the stationary phase, compared with the

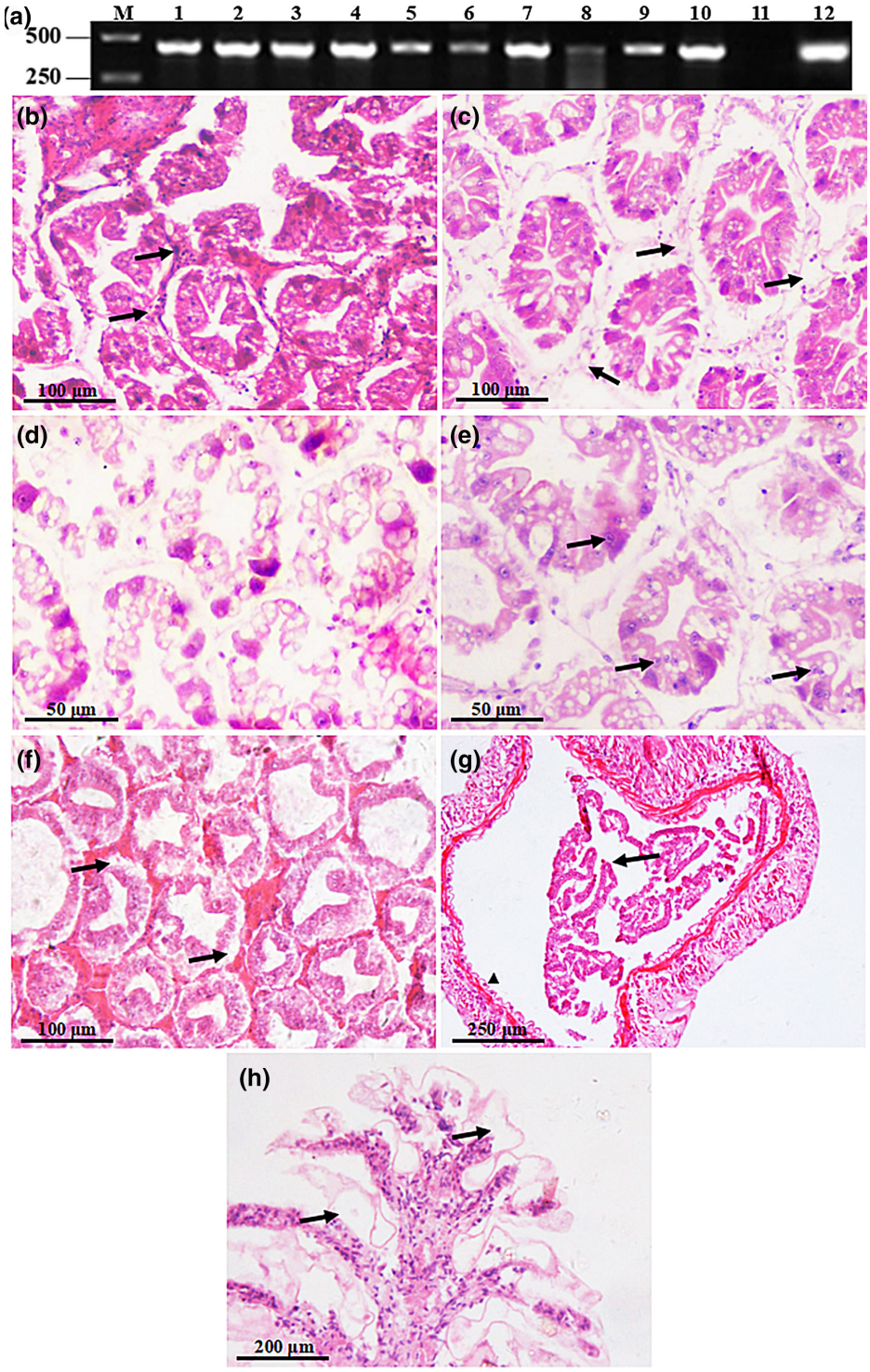


**Fig. 4.** The isolate TJA114 is the aetiological agent of the shrimp disease. (a) Agarose gel electrophoresis of PCR products of the *toxR* gene from the suspected *V. parahaemolyticus* isolates. M, Marker (unit, bp); 1–5, *toxR* gene test results of *V. parahaemolyticus* in the hepatopancreas of five shrimps in the $1\times10^{8}$ c.f.u. $ml^{-1}$ challenge group; 6–10, *toxR* gene test results of *V. parahaemolyticus* in the hepatopancreas of five shrimps in the $1\times10^{7}$ c.f.u. $ml^{-1}$ challenge group; 11, negative control; 12, positive control (the TJA114 isolate *toxR* gene). (b) Haemocyte infiltration in the hepatopancreas (arrows). (c) Increased intertubular space in the hepatopancreas (arrows). (d) Hypervacuolization of hepatopancreas cells. (e) Karyopyknosis in the hepatopancreas (arrows). (f) Sloughing of hepatopancreas cells from the basement membrane (arrows). (g) Intestinal epithelium collapse (arrow) and proliferating cells on the basement membrane of the intestine (arrowhead). (h) Gill filaments were swollen and epithelial cells separated from gill membranes (arrows).

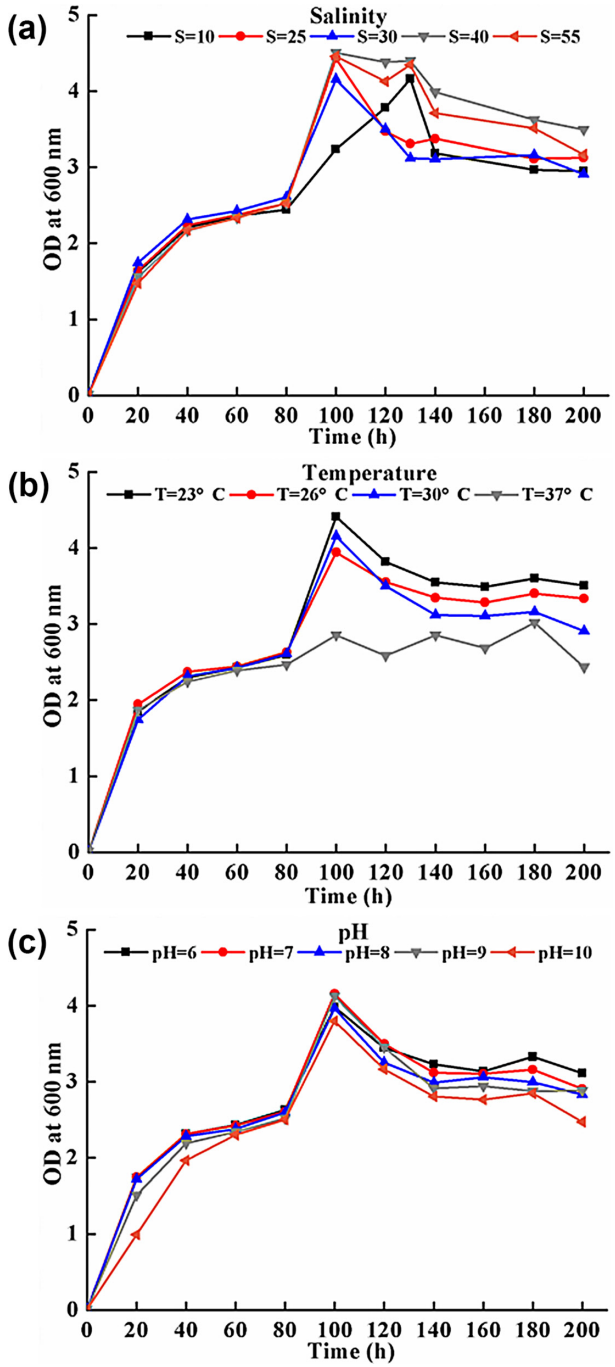


**Fig. 5.** Artificial growth curves of the TJA114 isolate. (a) Growth curve under salinity of 10–55 p.p.t. (b) Growth curve under temperature 23–37°C . (c) Growth curve under pH 6–10.

negative control (Fig. S2d, A10; Table S2), indicating that these substrates are beneficial for this isolate to cope with the alkaline environment. Many synthesis pathways of these substrates were identified in the genome annotation (Fig. 3). Taken together, these phenotype characteristics confirmed the predicted function notations from the genome data.

## DISCUSSION

In this study, one dominant bacterial strain was isolated from the hepatopancreas of diseased *P. vannamei* and identified as a non-AHPND *V. parahaemolyticus* that did not carry the *pirAB* genes. The analysis of phenotypic and genomic characterization of the *V. parahaemolyticus*, TJA114, revealed a combination of strategies that might empower its niche adaptation and pathogenic mechanism.

*V. parahaemolyticus* TJA114 caused the typical symptoms of vibriosis, presenting pathological lesions in multiple organs, which are similar to *P. vannamei* infected by previously reported non-AHPND *V. parahaemolyticus* strains [4, 12]. The observed lesions caused by the TJA114 isolate (Fig. 4b–h) were different from those of AHPND, whose typical histopathological changes seem to be limited to the hepatopancreas including exfoliated epithelial cells, expended chromatophores and hypertrophic nuclei [11, 69]. The discrepancies of the characteristic pathological changes between AHPND and the non-AHPND *V. parahaemolyticus* causing diseases in shrimps can be explained by the comparative genomics analysis to a certain extent. The *V. parahaemolyticus* TJA114 genome encoded many putative secreted proteases (Table S4) probably involved in destroying the chitin, lipid and protein structure of multiple organs, such as the hepatopancreas, gastrointestinal tract and gills. This was further confirmed by the pathohistological study in the recursive infection experiment (Fig. 4b–h). In addition, the dedicated protein secretion systems (Fig. 3) might secrete virulence factors from the cytosol of the bacteria into host cells or the host environment leading to histopathological lesions of *P. vannamei*. The invasiveness could be reflected by the ability of its motility, adhesion, biofilm formation, extracellular proteases secretion and haemolysin secretion.

*tdh* and *trh* genes encoding TDH and TRH responsible for the haemolytic activity and enterotoxicity often exist in clinical *V. parahaemolyticus* strains causing human disease [10, 53]. But the absence of *tdh* and *trh* genes could not exclude the probability of haemolysis by *V. parahaemolyticus* when invading hosts, because a clinical *V. parahaemolyticus* without *tdh* and *trh* genes isolated from acute diarrhoeal patients exhibited haemolytic activity to human erythrocytes [6, 44]. This phenomenon has been attributed to another haemolysin, TLH, encoded by the *tlh* gene [6]. In this study, although TJA114 did not harbour *tdh* and *trh* genes, once combining with the lecithin that is present in most living organisms, the *tlh* gene might have a similar effect to the two genes conferring the haemolytic activity [44].

AHPND-causing *V. parahaemolyticus* becomes virulent by acquiring a 70 kb plasmid (pVA1) encoding the binary PirAB toxins [11]. Some argued that the PirAB toxins are the primary virulence factors of AHPND-causing bacteria that mainly target the hepatopancreas of shrimp and damage the B (blister), E (embryonic), F (fibrillar) and R (resorptive) cells, resulting in dysfunction of the hepatopancreas and massive mortalities of shrimps [11]. Compared with AHPND-causing *V. parahaemolyticus*, the isolate TJA114 did not harbour a

type of plasmid like pVA1 nor, thus, *pirAB* genes, and consequently exhibited a different pathogenic mechanism, clinical symptoms and histological lesions, compared with the AHPND-causing *V. parahaemolyticus* strain. These findings provided the basis for the diagnosis of *V. parahaemolyticus* infection in shrimps.

Although the bacterium *V. parahaemolyticus* is a common pathogen, this isolate TJA114 should arouse much attention, because of its strong niche adaptability. This adaptability is reflected in the extensive utilization of nutrients, the diversity of metabolic pathways and the resistance to adverse environmental factors.

The extensive utilization of various carbohydrates, amino acids and substrates (Fig. S2a–d, Table S2) in the *V. parahaemolyticus* TJA114 was reflected in the genomic characteristics, including a variety of metabolic pathways (Fig. 3). The *V. parahaemolyticus* TJA114 can utilize more carbon sources than non-AHPND *V. parahaemolyticus* 20100612001 isolated from the hepatopancreas of diseased *P. vannamei* from Beihai, Guangxi province, China [12]. Of note, the TJA114 isolate can use malic acid as the only carbon source (Fig. S2a, C03; Table S2). But an AHPND-causing *V. parahaemolyticus*, EMS 13-028/A3, a human clinical *V. parahaemolyticus*, RIMD2210633, and an environmental *V. parahaemolyticus*, LM5312, cannot use malic acid [70]. The metabolic pathways of a variety of substances identified in the genome indicated its strong environmental suitability, which was confirmed by the PM assays of the osmolytes and pH plates. These metabolic functions for the abundant substances can give this *V. parahaemolyticus* a competitive advantage over other less metabolically capable bacteria, both in the aquaculture environment and within the target organs of target marine organisms such as shrimps. The presence of more plasmids, various stress adaptation factors, an array of sigma factors and anti-sigma factors, chaperones and TCSs in the *V. parahaemolyticus* TJA114 genome may ensure it is adaptable to environmental pressures, such as temperature fluctuation, pH changes, osmolarity variation and oxidative stress, as well as the responsive reactions of hosts.

The artificial growth curve of this *V. parahaemolyticus* indicated the organism's wide tolerance to environmental conditions (Fig. 5a–c). The short latent phase (Fig. S1) and long plateau phase (Fig. 5a–c) displayed on its growth curve may contribute to a short incubation period of shrimp diseases caused by the bacteria, usually resulting in acute outbreaks and high mortality. The secondary growth between 80 and 100 h on the growth curve indicated that this strain has the regulatory mechanism of carbon catabolite repression, by which the presence of a preferred substrate prevents gene expression required for the utilization of secondary carbon sources. This regulatory mechanism enables bacteria to increase their fitness by optimizing growth rates in the natural environments of complex mixtures of nutrients [70], increasing their chance to survive as a potential pathogen. When lacking glucose- and trehalose-phosphotransferase systems, *V. parahaemolyticus* strains cannot utilize the regulatory mechanism of carbon catabolite repression [71].

Aquatic bacteria with strong environmental adaptability often harbour an array of antibiotic-resistance determinants to resist the antibiotics that might be present in the aquaculture ecosystems [59]. The *V. parahaemolyticus* TJA114 could be considered as a multidrug-resistant isolate with resistance to tetracyclines, nitrofurans and penicillins, according to the results of antimicrobial-susceptibility test (Table 2). Accordingly, its drug-resistant mechanism, such as tetracycline efflux pump Tet35 (VP_GM003003), multidrug-resistant efflux pump NorM (VP_GM003344), multidrug-resistant proteins including EmrB (VP_GM000204), EmrD (VP_GM000275), MdtL (VP_GM000535, VP_GM001599), nitroreductase NfnB (VP_GM001616) and metallo-$\beta$-lactamase K07576 (VP_GM002081), were revealed by the genomic analysis. With an exception that the TJA114 isolate exhibited tetracycline resistance, this isolate demonstrated a similar antimicrobial spectrum to most AHPND-causing and non-AHPND *V. parahaemolyticus* strains isolated from seafood samples and diseased shrimps [72, 73]. Notably, the TJA114 isolate showed varying degrees of resistance to 7 of 19 antimicrobial agents recommended by the Centers for Disease Control and Prevention (CDC) for the treatment of *Vibrio* spp. [74], which indicates that it has gradually become insensitive to the quick-acting drugs for the treatment of *V. parahaemolyticus* and should be a cause for alarm.

In summary, phenotypic profiles of the *V. parahaemolyticus* TJA114 including pathogenicity, growth characteristics and nutritional requirements were investigated, and the isolate's genomic characteristics revealed the pathogenic mechanism and strong niche adaptability. Although AHPND-causing *V. parahaemolyticus* is still an important pathogen and has attracted much attention, in this study, we found that the non-AHPND *V. parahaemolyticus* strain is highly pathogenic and has a strong environmental adaptability. If such pathogens are not taken seriously, they may cause significant economic losses. Our results provide a basis for the deeper understanding of virulence factors and the formulation of better control strategies of *V. parahaemolyticus* infection in shrimps.

Funding information
This study was partially supported by the Innovation Team of Tianjin Fisheries Research System (ITTFRS2017009), the Scientific Programs of Tianjin City (19JCTPJC60100), the Science and Technology Innovation Project of Shandong province (2018SDKJ0406-4), the Science and Technology Project in the Field of Social Development in Tianjin Binhai New Area (BHXQKJXM-SF-2018–34), and the Scientific Research and Innovation Project of Tianjin Agricultural University in 2019 (2019XY038).

Author contributions
X. Z., performed the experiments, discussed the results and wrote the paper; J. S. and Y. Y. S., conceived and supervised all steps of the study and provided a critical review of the final version of the manuscript; F. C. and A. L., performed the experiments; H. Q. and L. C., were in charge of data curation; Y. H. and X. H., provided experimental animals and part of the study materials, respectively. All authors provided critical review and commentary.

Conflicts of interest
The authors declare that there are no conflicts of interest.

Ethical statement

All animal experiments were approved by the Animal Experiment Ethics Committee at Tianjin Agricultural University, China.

References


1. López-Cuadros I, García-Gasca A, Gomez-Anduro G, Escobedo-Fregoso C, Llera-Herrera RA *et al*. Isolation of the sex-determining gene *Sex-lethal* (*Sxl*) in *Penaeus* (*Litopenaeus*) *vannamei* (Boone, 1931) and characterization of its embryogenic, gametogenic, and tissue-specific expression. *Gene* 2018;668:33–47.
2. Thornber K, Verner-Jeffreys D, Hinchliffe S, Rahman MM, Bass D *et al*. Evaluating antimicrobial resistance in the global shrimp industry. *Rev Aquac* 2020;12:966–986.
3. Flegel TW. Historic emergence, impact and current status of shrimp pathogens in Asia. *J Invertebr Pathol* 2012;110:166–173.
4. Morales-Covarrubias MS, Cuéllar-Anjel J, Varela-Mejías A, Elizondo-Ovares C. Shrimp bacterial infections in Latin America: a review. *Asian Fish Sci* 2018;31S:76–87.
5. Lee C-T, Chen I-T, Yang Y-T, Ko T-P, Huang Y-T *et al*. The opportunistic marine pathogen *Vibrio parahaemolyticus* becomes virulent by acquiring a plasmid that expresses a deadly toxin. *Proc Natl Acad Sci USA* 2015;112:10798–10803.
6. Ghenem L, Elhadi N, Alzahrani F, Nishibuchi M, Nishibuchi M. *Vibrio parahaemolyticus*: a review on distribution, pathogenesis, virulence determinants and epidemiology. *Saudi J Med Med Sci* 2017;5:93–103.
7. Garin-Fernandez A, Glöckner FO, Wichels A. Genomic characterization of filamentous phage vB_Vpal_VP-3218, an inducible prophage of *Vibrio parahaemolyticus*. *Mar Genomics* 2020;53:100767.
8. Shanmugasundaram S, Mayavu P, Manikandarajan T, Suriva M, Eswar A *et al*. Isolation and identification of *Vibrio* sp. in the hepatopancreas of cultured white Pacific shrimp (*Litopenaeus vannamei*). *Int Lett Nat Sci* 2015;46:52–59.
9. Ananda Raja R, Sridhar R, Balachandran C, Palanisammi A, Ramesh S *et al*. Pathogenicity profile of *Vibrio parahaemolyticus* in farmed Pacific white shrimp, *Penaeus vannamei*. *Fish Shellfish Immunol* 2017;67:368–381.
10. Petronella N, Ronholm J. The mechanisms that regulate *Vibrio parahaemolyticus* virulence gene expression differ between pathotypes. *Microb Genom* 2018;4:e000182.
11. Soto-Rodriguez SA, Gomez-Gil B, Lozano-Olvera R, Bolan-Mejía M, Aguilar-Rendon KG *et al*. Pathological, genomic and phenotypical characterization of *Vibrio parahaemolyticus*, causative agent of acute hepatopancreatic necrosis disease (AHPND) in Mexico. *Asian Fish Sci* 2018;31S:102–111.
12. Zhang BC, Liu F, Bian HH, Liu J, Pan LQ *et al*. Isolation, identification, and pathogenicity analysis of a *Vibrio parahaemolyticus* strain from *Litopenaeus vannamei*. *Prog Fishery Sci* 2012;33:56–62.
13. Phiwsaiya K, Charoensapsri W, Taengphu S, Dong HT, Sangsuriya P *et al*. A natural *Vibrio parahaemolyticus* $\Delta pirA^{Vp}$ $pirB^{Vp}$+ mutant kills shrimp but produces neither $Pir^{Vp}$ toxins nor acute hepatopancreatic necrosis disease lesions. *Appl Environ Microbiol* 2017;83:e00680-17.
14. et al. Identification and toxicity analysis of a virulent *Vibrio parahaemolyticus* isolated from *Litopenaeus vannamei*. *Marine Fisheries* 2013;35:479–484.
15. Kwong JC, McCallum N, Sintchenko V, Howden BP. Whole genome sequencing in clinical and public health microbiology. *Pathology* 2015;47:199–210.
16. Tagini F, Greub G. Bacterial genome sequencing in clinical microbiology: a pathogen-oriented review. *Eur J Clin Microbiol Infect Dis* 2017;36:2007–2020.
17. Cao S, Geng Y, Yu Z, Deng L, Gan W *et al*. *Acinetobacter lwoffii*, an emerging pathogen for fish in *Schizothorax* genus in China. *Transbound Emerg Dis* 2018;65:1816–1822.
18. Hannula M, Hanninen ML. Phylogenetic analysis of *Helicobacter* species based on partial *gyrB* gene sequences. *Int J Syst Evol Microbiol* 2007;57:444–449.
19. Han Z, Sun J, Lv A, Sung Y, Shi H *et al*. Isolation, identification and characterization of *Shewanella algae* from reared tongue sole, *Cynoglossus semilaevis* Günther. *Aquaculture* 2017;468:356–362.
20. Bej AK, Patterson DP, Brasher CW, Vickery MC, Jones DD *et al*. Detection of total and hemolysin-producing *Vibrio parahaemolyticus* in shellfish using multiplex PCR amplification of *tl*, *tdh* and *trh*. *J Microbiol Methods* 1999;36:215–225.
21. Lai HC, Ng TH, Ando M, Lee C-T, Chen I-T *et al*. Pathogenesis of acute hepatopancreatic necrosis disease (AHPND) in shrimp. *Fish Shellfish Immunol* 2015;47:1006–1014.
22. Xian YY, Wei S, Yu C, Li ZY, MY Y. Novel multiplex polymerase chain reaction assay to detect virulence-related genes in *Vibrio parahaemolyticus*. *Mod Food Sci Technol* 2015;31:309–315.
23. Ardui S, Ameur A, Vermeesch JR, Hestand MS. Single molecule real-time (SMRT) sequencing comes of age: applications and utilities for medical diagnostics. *Nucleic Acids Res* 2018;46:2159–2168.
24. Zhou Y, Liang Y, Lynch KH, Dennis JJ, Wishart DS. PHAST: a fast phage search tool. *Nucleic Acids Res* 2011;39:W347–W352.
25. Kanehisa M, Goto S, Hattori M, Aoki-Kinoshita KF, Itoh M *et al*. From genomics to chemical genomics: new developments in KEGG. *Nucleic Acids Res* 2006;34:D354–D357.
26. Li W, Jaroszewski L, Godzik A. Tolerating some redundancy significantly speeds up clustering of large protein databases. *Bioinformatics* 2002;18:77–82.
27. Eichinger V, Nussbaumer T, Platzer A, Jehl M-A, Arnold R *et al*. EffectiveDB – updates and novel features for a better annotation of bacterial secreted proteins and type III, IV, VI secretion systems. *Nucleic Acids Res* 2016;44:D669–D674.
28. Chen L, Xiong Z, Sun L, Yang J, Jin Q. VFDB 2012 update: toward the genetic diversity and molecular evolution of bacterial virulence factors. *Nucleic Acids Res* 2012;40:D641–D645.
29. Jia B, Raphenya AR, Alcock B, Waglechner N, Guo P *et al*. CARD 2017: expansion and model-centric curation of the comprehensive antibiotic resistance database. *Nucleic Acids Res* 2017;45:D566–D573.
30. Maralit BA, Jaree P, Boonchuen P, Tassanakajon A, Somboonwiwat K. Differentially expressed genes in hemocytes of *Litopenaeus vannamei* challenged with *Vibrio parahaemolyticus* $_{AHPND}$ ($VP_{AHPND}$) and $VP_{AHPND}$ toxin. *Fish Shellfish Immunol* 2018;81:284–296.
31. Deng Y, Su Y, Liu S, Guo Z, Cheng C *et al*. Identification of a novel small RNA *srvg23535* in *Vibrio alginolyticus* ZJ-T and its characterization with phenotype microarray technology. *Front Microbiol* 2018;9:2394.
32. Buchanan RE, Gibbons NE. *Bergey's Manual of Determinative Bacteriology*, 8th edn. Baltimore, MA: Williams and Wilkins; 1974.
33. Liu L, Xiao J, Zhang M, Zhu W, Xia X *et al*. A *Vibrio owensii* strain as the causative agent of AHPND in cultured shrimp, *Litopenaeus vannamei*. *J Invertebr Pathol* 2018;153:156–164.
34. Jeon HJ, Noda M, Matoba Y, Kumagai T, Sugiyama M. Crystal structure and mutagenic analysis of a bacteriocin immunity protein, Mun-im. *Biochem Biophys Res Commun* 2009;378:574–578.
35. Gerth U, Krüger E, Derré I, Msadek T, Hecker M. Stress induction of the *Bacillus subtilis clpP* gene encoding a homologue of the proteolytic component of the Clp protease and the involvement of ClpP and ClpX in stress tolerance. *Mol Microbiol* 1998;28:787–802.
36. Li X, Zeng Y, Gao Y, Zheng X, Zhang Q *et al*. The ClpP protease homologue is required for the transmission traits and cell division of the pathogen *Legionella pneumophila*. *BMC Microbiol* 2010;10:54.
37. Fu S, Wang L, Tian H, Wei D, Liu Y. Pathogenicity and genomic characterization of *Vibrio parahaemolyticus* strain PB1937 causing shrimp acute hepatopancreatic necrosis disease in China. *Ann Microbiol* 2018;68:175–184.
38. McCarter LL. Polar flagellar motility of the *Vibrionaceae*. *Microbiol Mol Biol Rev* 2001;65:445–462.
39. Aagesen AM, Häse CC. Sequence analyses of type IV pili from *Vibrio cholerae*, *Vibrio parahaemolyticus*, and *Vibrio vulnificus*. *Microb Ecol* 2012;64:509–524.

40. Lee K-J, Lee NY, Han Y-S, Kim J, Lee K-H *et al*. Functional characterization of the IlpA protein of *Vibrio vulnificus* as an adhesin and its role in bacterial pathogenesis. *Infect Immun* 2010;78:2408–2417.
41. Krachler AM, Ham H, Orth K. Outer membrane adhesion factor multivalent adhesion molecule 7 initiates host cell binding during infection by Gram-negative pathogens. *Proc Natl Acad Sci USA* 2011;108:11614–11619.
42. Yildiz FH, Visick KL. *Vibrio* biofilms: so much the same yet so different. *Trends Microbiol* 2009;17:109–118.
43. Sudheesh PS, Xu H-S. Pathogenicity of *Vibrio parahaemolyticus* in tiger prawn *Penaeus monodon* Fabricius: possible role of extracellular proteases. *Aquaculture* 2001;196:37–46.
44. Wang R, Zhong Y, Gu X, Yuan J, Saeed AF *et al*. Corrigendum: the pathogenesis, detection, and prevention of *Vibrio parahaemolyticus*. *Front Microbiol* 2015;6:437.
45. Weaver EA, Wyckoff EE, Mey AR, Morrison R, Payne SM. FeoA and FeoC are essential components of the *Vibrio cholerae* ferrous iron uptake system, and FeoC interacts with FeoB. *J Bacteriol* 2013;195:4826–4835.
46. Bach FH. Heme oxygenase-1: a therapeutic amplification funnel. *FASEB J* 2005;19:1216–1219.
47. Sandkvist M. Type II secretion and pathogenesis. *Infect Immun* 2001;69:3523–3535.
48. Chernyatina AA, Low HH. Core architecture of a bacterial type II secretion system. *Nat Commun* 2019;10:5437.
49. Bhattacharjee RN, Park KS, Kumagai Y, Okada K, Yamamoto M *et al*. VP1686, a *Vibrio* type III secretion protein, induces Toll-like receptor-independent apoptosis in macrophage through NF-κB inhibition. *J Biol Chem* 2006;281:36897–36904.
50. Burdette DL, Seemann J, Orth K. *Vibrio* VopQ induces PI3-kinase-independent autophagy and antagonizes phagocytosis. *Mol Microbiol* 2009;73:639–649.
51. Salomon D, Guo Y, Kinch LN, Grishin NV, Gardner KH *et al*. Effectors of animal and plant pathogens use a common domain to bind host phosphoinositides. *Nat Commun* 2013;4:2973.
52. Waddell B, Southward CM, McKenna N, DeVinney R. Identification of VPA0451 as the specific chaperone for the *Vibrio parahaemolyticus* chromosome 1 type III-secreted effector VPA0450. *FEMS Microbiol Lett* 2014;353:141–150.
53. Okada N, Iida T, Park KS, Goto N, Yasunaga T *et al*. Identification and characterization of a novel type III secretion system in trh-positive *Vibrio parahaemolyticus* strain TH3996 reveal genetic lineage and diversity of pathogenic machinery beyond the species level. *Infect Immun* 2009;77:904–913.
54. Kumar BK, Deekshit VK, Rai P, Shekar M, Karunasagar I *et al*. Presence of T3SS2$\beta$ genes in trh$^+$ *Vibrio parahaemolyticus* isolated from seafood harvested along Mangalore Coast, India. *Lett Appl Microbiol* 2014;58:440–446.
55. Backert S, Meyer TF. Type IV secretion systems and their effectors in bacterial pathogenesis. *Curr Opin Microbiol* 2006;9:207–217.
56. Hachani A, Wood TE, Filloux A. Type VI secretion and anti-host effectors. *Curr Opin Microbiol* 2016;29:81–93.
57. Yu Y, Fang L, Zhang Y, Sheng H, Fang W. VgrG2 of type VI secretion system 2 of *Vibrio parahaemolyticus* induces autophagy in macrophages. *Front Microbiol* 2015;6:168.
58. Deutscher J, Francke C, Postma PW. How phosphotransferase system-related protein phosphorylation regulates carbohydrate metabolism in bacteria. *Microbiol Mol Biol Rev* 2006;70:939–1031.
59. Wang Q, Yang M, Xiao J, Wu H, Wang X *et al*. Genome sequence of the versatile fish pathogen *Edwardsiella tarda* provides insights into its adaptation to broad host ranges and intracellular niches. *PLoS One* 2009;4:e7646.
60. Hayrapetyan H, Tempelaars M, Groot MN, Abee T. *Bacillus cereus* ATCC 14579 RpoN (sigma 54) is a pleiotropic regulator of growth, carbohydrate metabolism, motility, biofilm formation and toxin production. *PLoS One* 2015;10:e0134872.
61. Missiakas D, Mayer MP, Lemaire M, Georgopoulos C, Raina S. Modulation of the *Escherichia coli* $\sigma^E$ (RpoE) heat-shock transcription-factor activity by the RseA, RseB and RseC proteins. *Mol Microbiol* 1997;24:355–371.
62. Wösten MMSM, Van Dijk L, Veenendaal AKJ, De Zoete MR, Bleumink-Pluijm NMC *et al*. Temperature-dependent FlgM/FliA complex formation regulates *Campylobacter jejuni* flagella length. *Mol Microbiol* 2010;75:1577–1591.
63. Vasudevan P, Venkitanarayanan K. Role of the *rpoS* gene in the survival of *Vibrio parahaemolyticus* in artificial seawater and fish homogenate. *J Food Prot* 2006;69:1438–1442.
64. Liu T, Wang KY, Wang J, Chen DF, Huang XL *et al*. Genome sequence of the fish pathogen *Yersinia ruckeri* SC09 provides insights into niche adaptation and pathogenic mechanism. *Int J Mol Sci* 2016;17:557.
65. Nakayama H, Yoshida K, Ono H, Murooka Y, Shinmyo A. Ectoine, the compatible solute of *Halomonas elongata*, confers hyperosmotic tolerance in cultured tobacco cells. *Plant Physiol* 2000;122:1239–1247.
66. Tanaka Y, Kimura B, Takahashi H, Watanabe T, Obata H *et al*. Lysine decarboxylase of *Vibrio parahaemolyticus*: kinetics of transcription and role in acid resistance. *J Appl Microbiol* 2008;104:1283–1293.
67. Ongagna-Yhombi SY, Boyd EF. Biosynthesis of the osmoprotectant ectoine, but not glycine betaine, is critical for survival of osmotically stressed *Vibrio parahaemolyticus* cells. *Appl Environ Microbiol* 2013;79:5038–5049.
68. Le TTT, Mawatari K, Maetani M, Yamamoto T, Hayashida S *et al*. VP2118 has major roles in *Vibrio parahaemolyticus* response to oxidative stress. *Biochim Biophys Acta* 2012;1820:1686–1692.
69. Lightner DV, Redman RM, Pantoja CR, Tran L. Early mortality syndrome affects shrimp in Asia. *Glob Aquacul Advocate* 2012;15:40.
70. Williams SL, Jensen RV, Kuhn DD, Stevens AM. Analyzing the metabolic capabilities of a *Vibrio parahaemolyticus* strain that causes early mortality syndrome in shrimp. *Aquaculture* 2017;476:44–48.
71. Stülke J, Hillen W. Carbon catabolite repression in bacteria. *Curr Opin Microbiol* 1999;2:195–201.
72. Tan CW, Rukayadi Y, Hasan H, Thung TY, Lee E *et al*. Prevalence and antibiotic resistance patterns of *Vibrio parahaemolyticus* isolated from different types of seafood in Selangor, Malaysia. *Saudi J Biol Sci* 2020;27:1602–1608.
73. Jia D, Shi C, Huang J, Zhang Q, Wan X *et al*. Identification and pathogenicity analysis of bacterial pathogen associated with acute hepatopancreatic necrosis disease (AHPND) in the Pacific shrimp *Litopenaeus vannamei*. *Prog Fishery Sci* 2018;39:103–111.
74. Shaw KS, Rosenberg Goldstein RE, He X, Jacobs JM, Crump BC *et al*. Antimicrobial susceptibility of *Vibrio vulnificus* and *Vibrio parahaemolyticus* recovered from recreational and commercial areas of Chesapeake Bay and Maryland Coastal Bays. *PLoS One* 2014;9:e89616.